

# An initial numerical investigation of the extent of sea-ice ridging

GREGORY M. FLATO AND WILLIAM D. HIBLER, III

*Thayer School of Engineering, Dartmouth College, Hanover, NH 03755, U.S.A.*

**ABSTRACT.** A two-level, viscous-plastic, sea-ice model is modified to allow ridged and unridged ice to be treated separately. This is accomplished by introducing a third continuity equation with additional terms to transform level ice into ridged ice during deformation. The standard model is run for three years using observed forcing from 1981–83, along with three sensitivity runs, to investigate the role of strength parameterization and energetically consistent deformation on ridge production. As expected, most of the ridging occurs near the coast, with the highest ridged-ice fraction produced off the Canadian archipelago and northern Greenland coast. The sensitivity studies indicate that, although the ridged-ice fraction is very sensitive to the strength parameterization, the lead fraction and total ice volume are much less affected. Requiring the deformation to be energetically consistent with the assumed yield curve almost doubles the amount of ridged ice produced.

## INTRODUCTION

The formation of leads and pressure ridges in polar pack ice provides the mechanism by which large-scale sea-ice dynamics interacts with smaller-scale mechanical processes to affect the local thickness distribution. In essence, large-scale deformation, driven by winds and currents, manifests itself locally as either ridge formation (as ice floes are pressed one against another) or lead opening (as ice floes separate). Typically, the central pack ice has between 10 and 40% of its area covered by ridged ice with this fraction rising to near 100% in active shear zones near the coast. It is through these small-scale processes that the mechanical properties of ice are related to the large-scale mechanical properties of the ice pack. Ridging and lead opening also provide the mechanism for feedback between dynamic and thermodynamic evolution of the ice cover. In this case, ridging causes an increase in the average ice thickness, and a concomitant decrease in thermodynamic growth, whereas lead opening promotes enhanced thermodynamic growth and decay by exposing areas of open water to the atmosphere.

Numerical models of the polar sea-ice cover have typically been compared to observations based on mean ice thickness; however, observations of the polar ice pack generally distinguish between ridged ice and level ice—ridged ice having been mechanically deformed to attain its thickness, and level ice having been formed by thermodynamic processes only. Observations of this type have been made while crossing the ice on dog sled (e.g. Koerner, 1973), from airborne laser profilometry (e.g. Hibler and others, 1974), and from submarine sonar transects (e.g. McLaren, 1989). Numerical models have generally not made this distinction and, therefore, compar-

isons of ridged-ice versus level-ice fractions cannot be made. Although small-scale, short-term simulations with a four-level model have been done (personal communication from R. Pritchard), the work described in this paper represents a first attempt to separate ridged and unridged ice in a large-scale sea-ice model, and so provide some insight to guide later, more complete studies.

## NUMERICAL MODELING APPROACH

The essential features of a numerical sea-ice model are a dynamic portion, which involves a solution of the momentum equation to find the ice-velocity field, and a thermodynamic portion which calculates the growth or decay of the ice cover based on a surface heat budget. These two components are linked by a continuity equation which describes the evolution of the thickness field by advection and growth. In the present study, the dynamic portion of the model is the viscous-plastic formulation of Hibler (1979), with the thermodynamic portion described by Hibler (1980).

Following Hibler (1979), the momentum equation for sea ice is given in vector form by

$$m \frac{\partial \mathbf{u}}{\partial t} = -mf\mathbf{k} \times \mathbf{u} + \boldsymbol{\tau}_a + \boldsymbol{\tau}_w - mg\nabla H + \mathbf{F}, \quad (1)$$

where the non-linear momentum advection term has been neglected and  $m$  is the mass of ice per unit area,  $\mathbf{u}$  is the ice velocity,  $t$  is time,  $f$  is the Coriolis frequency,  $\mathbf{k}$  is the upward unit normal,  $\boldsymbol{\tau}_a$  and  $\boldsymbol{\tau}_w$  are forces (per unit area) due to air and water drag, respectively,  $g$  is the acceleration due to gravity,  $H$  is the sea surface dynamic height, and  $\mathbf{F}$  is the force (per unit area) due to

variations in internal ice stress. Note that here and in the remainder of the paper, bold-face characters represent vector quantities. The internal ice force is defined as the divergence of the internal ice-stress tensor, which is in turn obtained by treating the ice cover as a viscoplastic continuum with an elliptical yield curve (see Hibler, 1979, for details). The yield curve specifies the maximum stresses that can be supported before plastic flow ensues and is defined by the ice-pack compressive strength,  $p_{max}$ .

The original Hibler (1979) model employed a two-level thickness formulation wherein the ice cover was considered to be composed of two fractions: an open-water fraction (actually taken to include ice less than 0.5 m thick in the thermodynamic calculations) and an ice-covered fraction described by an average thickness. A reasonable strength parameterization for the two-level model was proposed by Hibler (1979) as

$$p_{max} = p^*h \exp\{-K(1 - A)\}, \tag{2}$$

where  $p^*$  and  $K$  are empirical constants taken to be  $27.5 \text{ kN m}^{-2}$  and 20, respectively,  $h$  is the average ice thickness (in meters) and  $A$  is the compactness (or ice-covered fraction, a number between 0 and 1). The value for  $p^*$  was determined by Hibler and Walsh (1982), based on comparisons with the observed drift of a Soviet ice station, whereas  $K$  is the same value used in previous studies with this model to reflect the sharp decrease in pack-ice strength with increasing open-water fraction.

The original Hibler (1979) model required two continuity equations, one for the ice thickness,  $h$ , and the other for the compactness,  $A$ . The present model, which can be thought of as an extension of the two-level scheme, separates the ice cover into two components — ridged and unridged, with separate continuity equations for each. Since the average thickness,  $h$ , can be thought of as the average ice volume per unit area, it can be decomposed as

$$h = h_r + h_l, \tag{3}$$

where  $h_r$  and  $h_l$  are the ridged and unridged (level) ice volumes per unit area. The continuity equations can then be written as

$$\frac{\partial h_r}{\partial t} = -\nabla \cdot (\mathbf{u}h_r) + G_{h_r} + S_r + Q_A h_l, \tag{4a}$$

$$\frac{\partial h_l}{\partial t} = -\nabla \cdot (\mathbf{u}h_l) + G_{h_l} - S_r - Q_A h_l, \tag{4b}$$

$$\frac{\partial A}{\partial t} = -\nabla \cdot (\mathbf{u}A) + G_A - Q_A, \tag{4c}$$

where  $G_{h_r}$ ,  $G_{h_l}$ , and  $G_A$  are thermodynamic growth rates for ridged ice, level ice, and open water, respectively.  $S_r$  is the rate of volume transfer from level to ridged ice; and  $Q_A$  is the additional rate of open-water creation required to make the deformation energetically consistent with the elliptical yield curve. These various source terms will be discussed more fully below.

The thermodynamic growth terms are the same as those described by Hibler (1980), with the total ice-growth rate  $G_h = G_{h_r} + G_{h_l}$  based on the total average thickness,  $h$ , and partitioned to the ridged and level ice fractions in proportion to their volume. The ridging

transfer term,  $S_r$ , acts as a sink of level ice and a source of ridged ice and is defined as

$$\begin{aligned} S_r &= -h_l(\nabla \cdot \mathbf{u}) \exp -K(1 - A), \quad \nabla \cdot \mathbf{u} \leq 0; \\ S_r &= 0, \quad \nabla \cdot \mathbf{u} > 0. \end{aligned} \tag{5}$$

That is, the rate of ridge production is taken to be proportional to the level-ice volume, the negative divergence rate (i.e. the convergence rate), and the same exponential factor as in Equation (2) if there is a net convergence, and zero if there is a net divergence. The exponential factor ensures that ridge production is consistent with the strength parameterization. It is also consistent with one's intuition, since regions with a large open-water fraction (small  $A$ ) should experience less ridging during convergence, as leads can be closed up.

The open-water production rate,  $Q_A$ , was not included in the original Hibler (1979) model but is required to make the ice deformation energetically consistent with the assumed yield curve. Basically, this term is responsible for the creation of open-water area in Equation (4c) and ridged-ice volume in Equation (4a) in response to deviatoric (shearing) deformation. In other words, pure shearing deformation, although producing no net change in area, simultaneously creates open water and ridged ice as interlocking floes reorient themselves. This is required for energetic consistency since finite shear strength is assumed to result from the energy sink provided by ridge creation (see Rothrock, 1975, for a fuller discussion of this point). An expression for this additional rate of open-water production, consistent with the elliptical yield curve, was discussed briefly by Hibler (1984) and is given as

$$Q_A = 0.5K_A \left\{ \left[ (\dot{\epsilon}_{xx}^2 + \dot{\epsilon}_{yy}^2)1.25 + \dot{\epsilon}_{xy}^2 + 1.5\dot{\epsilon}_{xx}\dot{\epsilon}_{yy} \right]^{1/2} - |\dot{\epsilon}_{xx} + \dot{\epsilon}_{yy}| \right\}, \tag{6}$$

where  $\dot{\epsilon}_{xx}$ ,  $\dot{\epsilon}_{yy}$ , and  $\dot{\epsilon}_{xy}$  are the components of the strain-rate tensor (Hibler, 1980). The coefficient,  $K_A$ , was taken by Hibler (1984) to be a quadratic function of compactness; however, to be consistent with Equation (5),  $K_A$  is defined here as

$$K_A = \exp -K(1 - A). \tag{7}$$

It should be noted that the actual level-ice thickness ( $h_l$  divided by the fraction of area covered by level ice) should be used in Equations (4a) and (5); however, this would require an arbitrary specification of the ratio of ridged- to level-ice thickness, which has not been done. In this sense, the ridged-ice volume calculated by the present model is perhaps a lower bound. However, since the two-level formulation is a rather crude approximation to begin with, further refinements are probably not warranted. The idea here is to have an initial look at the spatial patterns of ridge production and the effect of strength parameterizations, not to make detailed quantitative comparisons with observations.

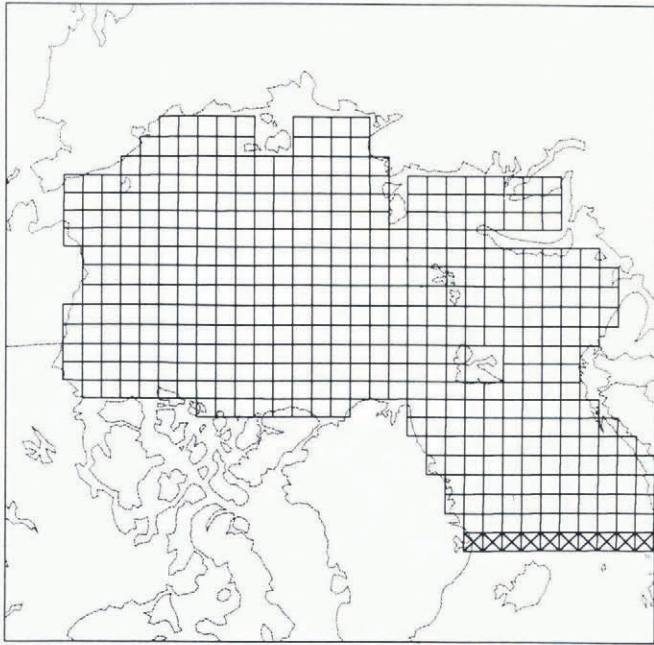


Fig. 1. Computational grid used in simulations. Grid cells are  $160 \text{ km}^2$  with cross-hatched cells indicating outflow boundaries.

## SIMULATION RESULTS

### Computational grid and forcing fields

The numerical results described in this section were obtained by applying the model to a  $160 \text{ km}$ -resolution Cartesian grid representing the Arctic Ocean, Barents Sea and parts of the Norwegian and Greenland seas as shown in Figure 1. The time step is one day. Lateral boundary conditions are “no-slip” at land boundaries and free outflow to the North Atlantic, as described by Hibler (1979), through the cross-hatched grid cells in the figure. The model results presented make use of forcing fields for the period January 1981 to December 1983; however, to ensure a reasonable initial state, the model was allowed a one year “spin-up” using the 1981 forcing.

The 1981–83 data set uses wind fields from the NCAR surface pressure analysis and the thermodynamic fields from the NASA analysis (personal communication from J. Walsh). The average annual oceanic heat flux and the geostrophic ocean currents (approximated by the average annual surface currents) are from the diagnostic ice–ocean calculation of Hibler and Bryan (1987).

### Standard simulation

The standard simulation used the original Hibler (1979) formulation, with ridges and leads produced only by convergence and divergence, that is with  $Q_A = 0$  in Equation (4). Figure 2 shows the average thickness, ridged-ice fraction, and ridged-ice volume per unit area for March 1983, as well as the average annual ridged-ice production for the three-year simulation period. Ridged-ice fraction is defined simply as the fraction of total volume composed of deformed ice,  $h_r/h$ . The thickness field in Figure 2a exhibits the same general pattern as the mean fields compiled by Bourke and Garret (1987), with relatively thick ice off northern Greenland and the Canadian

archipelago, thinning gradually across the Arctic Basin to the Siberian coast. However, the extremely thick ice off northern Greenland, observed by Bourke and Garret (1987) in the summer and fall, is not reproduced by the present model and may be due to limitations of the two-level formulation. It might be noted here that the more complete multi-level formulation employed by Hibler (1980) did produce much thicker ice in this region.

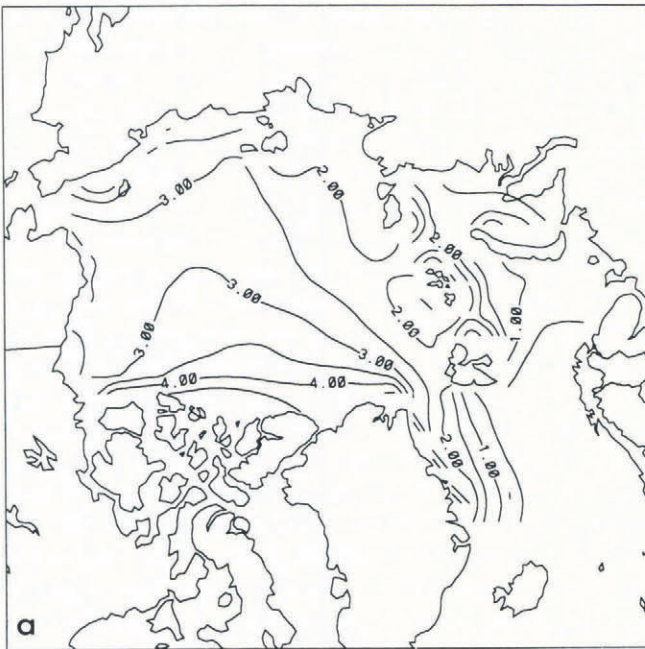
The ridged-ice patterns in Figure 2b support both intuition and observation in that the most heavily ridged ice occurs near the coasts, with relatively less ridging in the central pack. The volume per unit area, or effective thickness, of ridged ice for March 1983, shown in Figure 2c, can be compared to that summarized by Hibler and others (1974) for 1971 and 1973 when it was found to vary from  $0.4\text{--}0.6 \text{ m}$  in the central Arctic and  $0.7\text{--}1.4 \text{ m}$  near the Canadian archipelago. Since these observations included only those ridges over  $6.1 \text{ m}$  thick, whereas the present calculation includes all deformed ice, one would expect the calculated values to be larger. The comparison of instantaneous ridged-ice volume per unit area in Figure 2c to the average annual ridge production (also expressed as volume per unit area) in Figure 2d, illustrates the effect of advection on ridge distribution. As noted earlier, Figure 2d demonstrates that ridging occurs primarily within a narrow band near the coast; however, the intense ridge production off the north coasts of Greenland and Spitsbergen is not reflected in the instantaneous ridge intensity. Clearly what is happening is that ridges are produced as ice is forced through Fram Strait, and subsequently advected into the Greenland Sea.

Quantitative comparisons to observed areal ridge fraction require assumptions about the ratio of ridged- to unridged-ice thickness and the shape of a typical ridge. For example, reasonable assumptions regarding ice-ridge shape and thickness (namely: sail and keel are assumed to be triangular with side slopes of  $26^\circ$  and  $40^\circ$ , respectively; the keel depth is assumed to be four times the sail height; and the ridge thickness is taken as four times the level ice thickness — see, for example, Weeks and others, 1971) yield areal fractions of 13 to 21% on the surface and 29 to 42% on the underside, for the volume fractions of 20 to 30% produced by the model in the central Arctic. However, this is somewhat artificial and is probably not justified given the crudeness of the two-level formulation. Nonetheless, a brief review of some selected observations will be made here to provide a feel for actual conditions in the Arctic. It might be noted in passing that the multi-level thickness-distribution scheme, proposed by Thorndike and others (1975) and implemented by Hibler (1980), does provide a framework for making comparisons of both ridged versus unridged area, volume, and thickness distribution statistics. This approach is currently being investigated by the authors.

One of the most extensive data sets of observed ice thickness is that compiled by McLaren (1989), based on two submarine cruises along identical tracks across the Arctic in August of 1958 and 1970. McLaren (1989) analyzed the upward-looking sonar transect in two sections: one in the Canadian Basin region along  $155^\circ \text{ W}$  and one in the North Pole–Eurasian Basin region along  $25^\circ \text{ E}$ . The transect through the Canadian Basin region was found to have about 12% ridged ice, as a fraction of

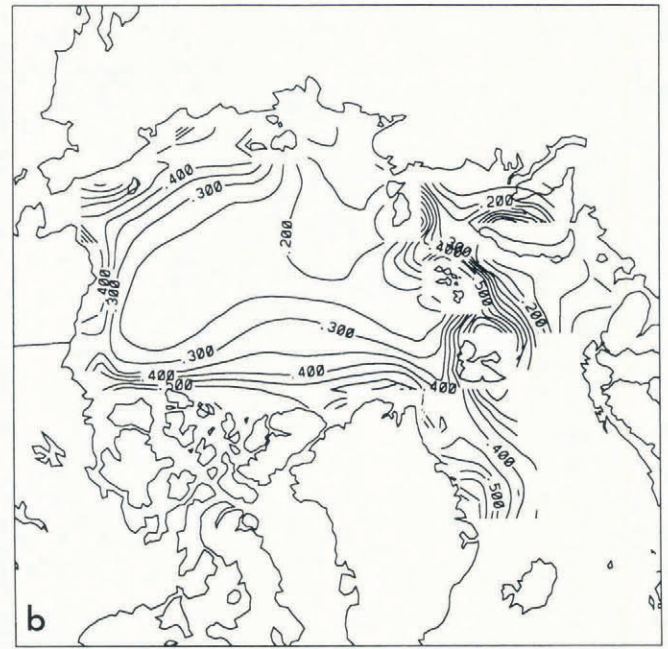
Total Ice Thickness. 1983

- MARCH



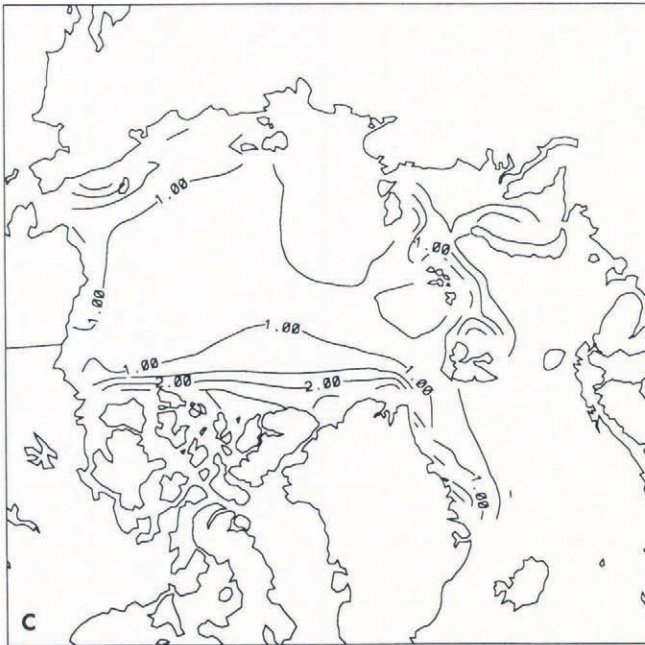
Ridged Ice Fraction. 1983

- MARCH



Ridged Ice Volume per unit Area. 1983

- MARCH



Average Annual Ridge Production

- MARCH

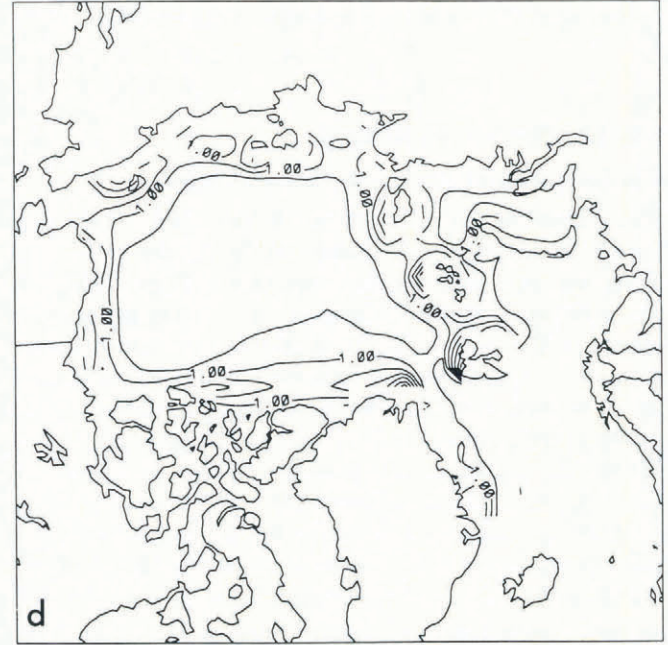


Fig. 2. Standard model results. (a) Total ice thickness (m) for March 1983. (b) Ridged ice-fraction (by volume) for March 1983. (c) Ridged-ice volume per unit area (m) for March 1983. (d) Annual ridge production averaged over three-year simulation period and expressed as volume per unit area (m). Note that most of the ridged ice is produced within about 300 km of the coast.

transect distance, in 1970 and about 22% in 1958. The Eurasian Basin region had 27% ridged ice in 1970 and 39% in 1958. A transect following almost the same route as the above mentioned submarine transects was made by dog sled during the British Trans-Arctic Expedition in 1968-69. Surface observations made during this expedition indicated about 10% newly-ridged ice in both the Canadian Basin and Eurasian Basin regions, with the figure rising to 15% in the Canadian Basin if multi-year

ridges are included (Koerner, 1973). These ridge fractions, although expressed as a fraction of transect distance, are probably quite close to areal fractions owing to the linear nature of ridge features. It is apparent, from even a cursory review such as this, that ridge intensity exhibits large variability, both spatially and temporally and, furthermore, that the ridge statistics one obtains from observations of ice thickness depend strongly on the definitions one uses to separate ridged from unridged ice.

**Sensitivity studies**

Ridge production in the two-level model is controlled largely by the strength parameterization and the requirement for energetic consistency during shear deformation. To investigate these effects, three sensitivity simulations were run: the first with half the normal compressive strength,  $p^*$ ; the second with twice the compressive strength; and the third with the standard compressive strength, but with the additional open-water creation,  $Q_A$ , required for energetic consistency. Note that the shear strength is proportional to the compressive strength and so the shear and compressive strengths are equally affected by the strength modifications. Since the spatial patterns of thickness build-up and ridged-ice fraction were not dramatically different in these sensitivity runs, only time-series of average quantities will be

shown here. These time-series also illustrate annual and interannual variability of the system as a whole.

The first two time-series, in Figure 3, show the average lead fraction (that is, the fraction of open-water area in regions with non-zero ice thickness) and average ridged-ice fraction over the entire domain for the three sensitivity runs and the standard simulation. Readily apparent in Figure 3a is the dramatic seasonal swing in lead area. The high strength simulation, with double the normal strength, exhibits somewhat less lead area and ridged ice since deformation is restricted. The low strength simulation allows more convergence and, hence, more ridged-ice and lead-area production. The case in which lead-area creation and ridging are allowed during shear deformation produces more lead area, as expected, with almost the same average lead fraction as the low strength case. However, the ridged-ice fraction for this case, in Figure 3b, is considerably larger than the low strength case. The reason for this is that ridged ice is

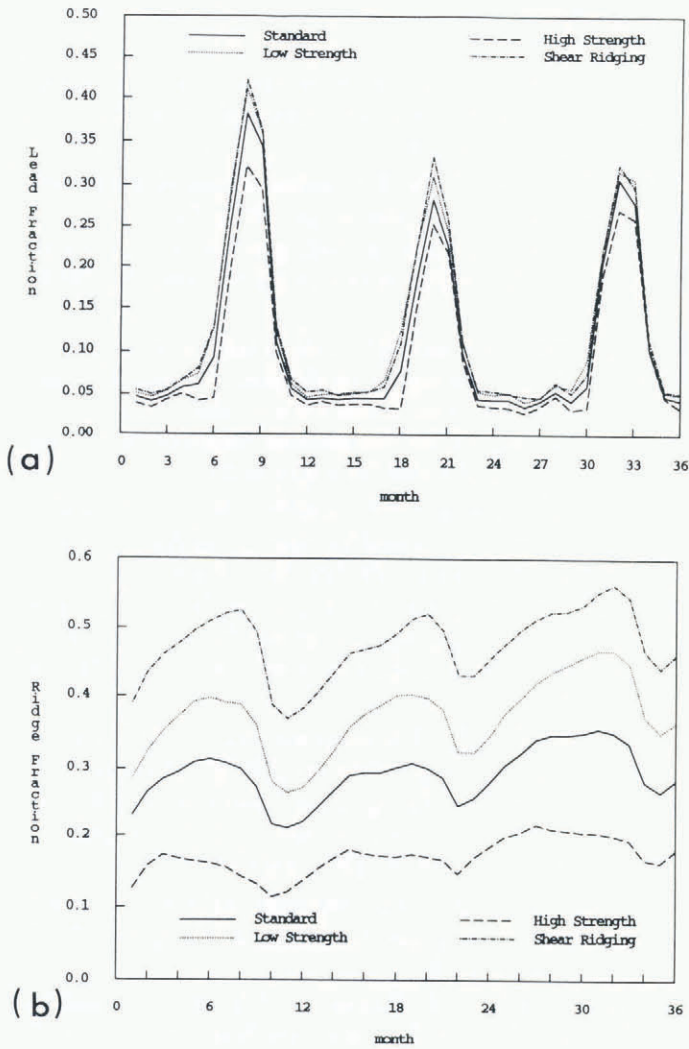


Fig. 3. (a) Time-series of average lead fraction (fraction of total area covered by open water in regions with non-zero ice thickness) over entire computational domain for simulation period 1981–83. (b) Time-series of average ridged-ice fraction (by volume) over entire computational domain for simulation period 1981–83. The lead fraction (and hence heat flux to the atmosphere) is relatively insensitive to the strength parameterization, in contrast to the ridged-ice fraction, which almost doubles with the inclusion of ridge production during shearing.

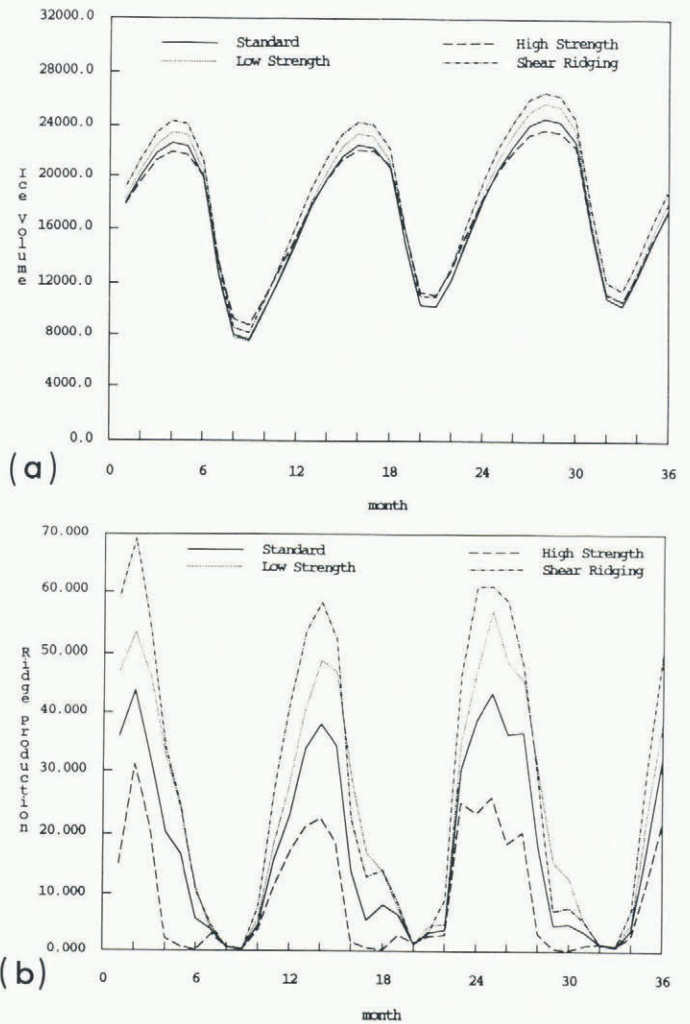


Fig. 4. (a) Time-series of total ice volume ( $\text{km}^3$ ) for simulation period 1981–83. (b) Time-series of monthly average ridge production ( $\text{km}^3\text{d}^{-1}$ ). Notice that the ridge production reaches a peak in January or February, whereas the ice volume continues to increase, due to thermodynamic growth, until about May. The reason for this is the suppression of ridge production in late winter as the pack ice becomes thicker and more compact and, hence, able to resist deformation.

created directly during shear and, in addition, some ridging occurs due to the lower strength associated with a larger fraction of open water (i.e. lower compactness in Equation (2)). It is interesting to note that the ridged-ice fraction in the energetically consistent case is almost double that of the standard case. It is also noteworthy that the ridged-ice fraction in 1983 is somewhat higher than in 1981 and, furthermore, that the seasonal cycle for each year in Figure 3b is almost identical to the seasonal cycle one obtains by integrating the model to equilibrium, repeating a given year's forcing over and over.

A final comparison is given in Figure 4, in which time-series of the total Arctic sea-ice volume and ridged-ice production for the four simulations are plotted. The general trend in the ice volume results is similar to the ridged-ice fraction results. However, the sensitivity is considerably less. This is primarily due to feedback between dynamics and thermodynamics, since enhanced dynamic thickness build-up inhibits thermodynamic growth and vice versa. Comparison of the ridged-ice production and total ice volume shows that the peak in ice-ridge production occurs in January or February, two to three months earlier than the peak in ice volume. This result illustrates the feedback between pack-ice strength and ridging in that an increase in strength, caused by an increase in thickness and compactness, makes further ridging more difficult.

## DISCUSSION AND CONCLUSIONS

The two-level sea-ice model is widely used and is able to reproduce average ice thicknesses and ice drift rather well, particularly in the central pack. However, this model is somewhat limited by the fact that only two variables, average thickness and compactness, are available to characterize the ice-pack strength. The details of the ice-thickness distribution — the relative fractions of thin, thick, and ridged ice — are thought to play an important role in determining the overall mechanical properties of the ice pack. Nonetheless, the simple extension of the scheme presented here, to allow calculation of the ridged- and level-ice fractions, shows considerable promise to provide at least a qualitative picture of the large-scale ridging process.

The three-year simulations discussed above exhibited the general pattern of more intense ridging near the coasts, particularly near the Canadian archipelago and northern Greenland, observed from aircraft, as well as the general thickness build-up patterns seen in compilations of submarine ice-thickness measurements. Quantitative comparisons to observations are made difficult both by differing definitions of ridged versus unridged ice and by the requirement to convert between volumetric ridged-ice fraction, calculated by the model, and the more usual areal ridged-ice fraction observed. Such comparisons are possible with a more complete multi-level thickness formulation and this approach is currently under investigation by the authors.

The sensitivity studies conducted here illustrated the dependence of calculated ridged-ice fraction on both pack-ice strength and the requirement for energetically consistent deformation. It was found that increasing strength resulted in less open-water creation and ridge

production due to overall restriction of the deformation. The energetically consistent case, while producing considerably more open water and ridged ice during deformation, exhibited only a slightly larger open-water fraction and ice volume on the whole. The reason for this is the feedback between open-water production and ice strength — increased open-water area reduces ice strength, allowing easier convergence and concomitant lead closing. It was noted that the energetically consistent case yielded almost double the ice-ridge volume of the standard case.

## ACKNOWLEDGEMENT

This work was supported by the U.S. Office of Naval Research under contract N00014-86-K-069.

## REFERENCES

- Bourke, R.H. and R.P. Garrett. 1987. Sea ice thickness distribution in the Arctic Ocean. *Cold Reg. Sci. Technol.*, **13**(3), 259–280.
- Hibler, W.D., III. 1979. A dynamic thermodynamic sea ice model. *J. Phys. Oceanogr.*, **9**(4), 815–846.
- Hibler, W.D., III. 1980. Modeling a variable thickness sea ice cover. *Mon. Weather Rev.*, **108**(12), 1943–1973.
- Hibler, W.D., III. 1984. The role of sea ice dynamics in modeling CO<sub>2</sub> increases. In Hansen, J.E. and T. Tikhonov, eds. *Climate processes and climate sensitivity*. Washington, DC, American Geophysical Union, 238–253. (Geophysical Monograph 29.)
- Hibler, W.D., III, and J.E. Walsh. 1982. On modeling seasonal and interannual fluctuations of Arctic sea ice. *J. Phys. Oceanogr.*, **12**(12), 1514–1523.
- Hibler, W.D., III, S.J. Mock and W.B. Tucker, III. 1974. Classification and variation of sea ice ridging in the western Arctic basin. *J. Geophys. Res.*, **79**(18), 2735–2743.
- Koerner, R.M. 1973. The mass balance of the sea ice of the Arctic Ocean. *J. Glaciol.*, **12**(65), 173–185.
- McLaren, A.S. 1989. The under-ice thickness distribution of the Arctic basin as recorded in 1958 and 1970. *J. Geophys. Res.*, **94**(4), 4971–4983.
- Rothrock, D.A. 1975. The energetics of the plastic deformation of pack ice by ridging. *J. Geophys. Res.*, **80**(33), 4514–4519.
- Thorndike, A.S., D.A. Rothrock, G.A. Maykut, and R. Colony. 1975. The thickness distribution of sea ice. *J. Geophys. Res.*, **80**(33), 4501–4513.
- Weeks, W.F., A. Kovacs and W.D. Hibler, III. 1972. Pressure ridge characteristics in the Arctic coastal environment. In Wetteland, S.S. and P. Bruun, eds. *Proceedings, the First International Conference on Port and Ocean Engineering under Arctic Conditions ... Aug. 23–30, 1971*. Trondheim, Technical University of Norway, 152–183.

*The accuracy of references in the text and in this list is the responsibility of the authors, to whom queries should be addressed.*